A Graph Signal Processing Approach to Direction of Arrival Estimation

1st Leandro A. S. Moreira
Graduate Program in Defense Engineering
Military Institute of Engineering (IME)
Rio de Janeiro, Brazil
leandromoreira75@gmail.com

2nd António L. L. Ramos
Department of Science and Industry Systems
University of South-Eastern Norway (USN)
Kongsberg, Norway
antonio.ramos@usn.no

3rd Marcello L. R. de Campos
Electrical Engineering Program
Federal University of Rio de Janeiro (UFRJ)
Rio de Janeiro, Brazil
campos@smt.ufrj.br

4th José A. Apolinário Jr.
Department of Electrical Engineering
Military Institute of Engineering
Rio de Janeiro, Brazil
apolin@ieee.org

5th Felipe G. Serrenho
Department of Electrical Engineering
Military Institute of Engineering
Rio de Janeiro, Brazil
felipe.serrenho@gmail.com

***Abstract*—This work presents a new approach, based on Graph Signal Processing, to estimate the direction of arrival (DoA) of an incoming narrowband signal hitting on an array of sensors. By building directed graphs related to both a uniform linear sensor array and a time series representing the signal at each sensor, we use the concepts of graph product and graph Fourier transform to form an objective function from the coefficients of the signal represented in an eigenvectors basis. Simulation results have shown that the method achieves estimations with competitive precision in comparison to classical DoA estimation methods, and good results being obtained even in presence of multipath and interfering. The proposed method is suitable for parallel implementations and its computational complexity tends to decrease when used repeatedly.**

***Index Terms*—Direction of arrival, array signal processing, Graph Fourier Transform, narrowband DoA estimation**

I. Introduction

Graph Signal Processing (GSP) develops tools for modeling massive amounts of data and their complex interactions [1]. In traditional spectral graph theory (SGT), eigenvalues (spectrum) and eigenvectors of the adjacency and Laplacian matrices of a given graph are used to analyze the structure of that graph [2]. In GSP, signals are processed over an irregular data domain, a graph representing signal plus structure. Interesting questions about GSP include concepts of translating a signal on a graph and simplifying sensor networks [3], [4]. While in classical signal processing a signal translation is implemented by performing a change of variables (time delay), in graph signal processing the idea of translation is naturally more challenging since it depends on what shall be defined as an ordered set of nodes [3]. Nevertheless, it is interesting to note that the use of spectral methods, which depend on the calculation of eigenvalues and eigenvectors of graphs, have already been proposed for the simplification of graphs [5]. For the same purpose, the concept of diffusion distance in graphs was applied [6], which is also used by [7] for the construction of a spectral method for data dimensionality reduction. That method was employed in [8] to locate a sound source in a controlled environment, without spatial information provided by a microphone array. The latter seems to be one of the first works to deal with a problem similar to DoA estimation, using the spectrum of a graph.

High-resolution narrowband DoA estimation sub-space methods, such as MUSIC [9] and ESPRIT [10], rely on the eigendecomposition of the autocorrelation matrix of the input signal. This paper proposes an approach to estimate the DoA of a signal impinging on a uniform linear sensor array, by means of concepts such as graph product and Graph Fourier Transform (GFT). The array of sensors is interpreted as a graph and a GFT is applied on the input signals stacked as a vector, $\mathbf{x}$. By obtaining a suitable *adjacency matrix* $\mathbf{A}$ such that, for a single sinusoidal incoming signal, we could write $\mathbf{x} = \mathbf{A}\mathbf{x}$. We devise a DoA estimation algorithm that takes advantage of the fact that vector $\mathbf{x}$, in this particular case, is an eigenvector of matrix $\mathbf{A}$. Our experimental results show that this method is also valid for a more realistic scenario using a modulated signal, and also including other factors such as noise, multipath, and interference.

The rest of the paper is organized as follows. Section II presents the fundamentals of GSP followed by a description of the graph models of a uniform linear array in Section III. Section IV addresses the DoA estimation problem, while simulation results and conclusions are summarized in sections V and VI, respectively.

II. Fundamentals of Graph Signal Processing

A graph $G = (V, E, W)$ is a set of nodes V and edges E, associated with a weight function W that represents a measure of similarity between connected nodes. Data or signals on a graph

This work was financed in part by the Coordenação de Aperfeiçoamento de Pessoal de Nível Superior (CAPES), Brazil – Financing Code 88881.117868/2016-01, by the Conselho Nacional de Desenvolvimento Científico e Tecnológico (CNPq), Brazil, and by Diku, Norway.

978-9-0827-9703-9/19/$31.00 ©2019 IEEE

are defined as a collection of samples $\mathbf{s} = \{s_1, s_2, ..., s_N\}$, associated to each node $V = \{v_1, v_2, ..., v_N\}$ of the graph. Operations such as shifts, filtering, and Fourier transform can be define by means of graph Laplacian or adjacency matrices. The Laplacian matrix is employed in the case of undirected graphs with real and non-negative weights [3], whereas adjacency matrix is more usual for directed graphs, as is the case described in this paper. For that reason, operators used in the discussion that follows are devised based on an adjacency matrix. For further information refer to [3], [4].

A. Graph Fourier Transform

The classical Fourier transform consists in writing a given function as a weighted sum of complex exponentials, the eigenfunctions of the one-dimensional Laplace operator. The discrete-time Fourier transform (DTFT) is based on orthonormal eigenvectors computed by diagonalizing the cyclic shift matrix $\mathbf{C}$ [11]. The eigenvalues associated to these eigenvectors are the frequencies of the transform. A graph Fourier transform (GFT) is defined similarly, by using the eigenvectors of the adjacency matrix $\mathbf{A}$, which then become the frequency components of the transformation. Thus, given that the eigendecomposition $\mathbf{A} = \mathbf{V}\mathbf{\Lambda}\mathbf{V}^{-1}$ exists, $\mathbf{\Lambda}$ being the diagonal matrix whose diagonal entries are the eigenvalues of $\mathbf{A}$ and $\mathbf{V}$ the matrix whose columns are the eigenvectors of $\mathbf{A}$, the GFT of a signal $\mathbf{s}$ is computed by $\hat{\mathbf{s}} = \mathbf{V}^{-1}\mathbf{s}$ such that the graph signal can be written as $\mathbf{s} = \hat{s}_1\mathbf{v}_1 + \hat{s}_2\mathbf{v}_2 + \cdots + \hat{s}_N\mathbf{v}_N$ [4]. Note from the previous expression that vector $\mathbf{v}_n$ is the n-th eigenvector of matrix $\mathbf{A}$. Also, whenever the adjacency matrix is Hermitian, there exists a unitary eigenvector matrix $\mathbf{V}$ such that $\mathbf{V}^{-1} = \mathbf{V}^{\mathrm{H}}$ [12].

III. Graph Model for Narrowband Signals

Consider, without loss of generality, a uniform linear array (ULA) of M microphones as depicted in Fig. 1, where the processing block after the A/D converter is an analytical bandpass filter centered at ω_0, the central frequency of the incoming narrowband signal. This block is designed to filter out the negative portion of the input signal spectrum, such that a multiplication by a complex exponential $e^{-j\omega_0\tau}$ results in a delay of τ samples. In the simple case of $x_m(t)$ a single cosine, the signal from the m-th microphone after the bandpass filter can be expressed as $x_m(k) = e^{j\omega_0 k}e^{-j\omega_0(m-1)\tau}$. Assuming an angle θ (the DoA), the delay in number of samples is computed by $\tau = d\cos(\theta)f_s/v_s$, where d is the distance between two consecutive microphones, f_s is the sampling frequency, and v_s is the speed of sound. The DoA estimation problem consists of obtaining an estimate of angle θ from the delays between microphones and other signal parameters. Even though such problem can be solved by simple beamscan algorithms such as Delay-and-Sum (or Bartlet beamformer) [13], or by spectral based algorithms such as MUSIC [9] and ESPRIT [10], our motivation here is to propose a new approach to estimate DoA based on graph Fourier transform. The idea is to model both the array sensor (ULA) and the time series (signal) as directed graphs and to compute the GFT of the graph product obtained by relating space and time dimensions. This process is described in the following.

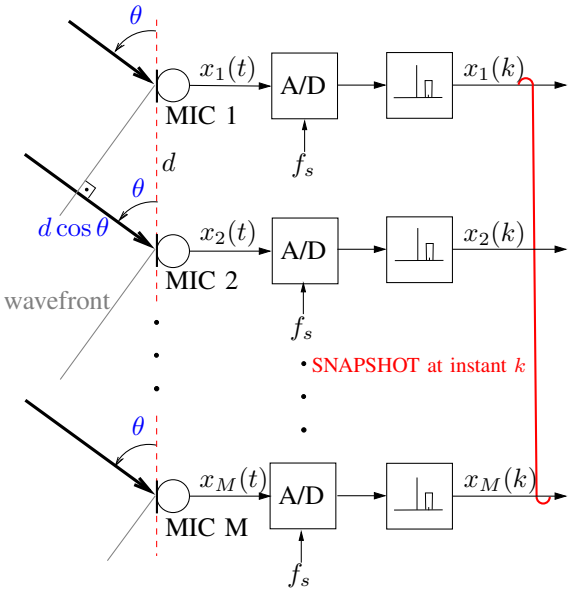

Fig. 1: Uniform Linear Array with M microphones.

A. Space-domain Adjacency Matrix

The relationships between signals from the M microphones in the ULA (space dimension) are modeled by using a sparse directed graph, in which each microphone is connected only with its closest neighbours, except for the sensors in the extremities, which are also connected to each other. So, in this equation there are only two nonzero elements per row. Other representations do exist, which yield adjacency matrices with different structures and degrees of sparsity.

In the adjacency matrix $\mathbf{A_1}$, the neighborhood criterion is given by delays or advances, and the relationship between microphones is determined by complex exponential, $z = e^{j\omega_0\tau}$ and its conjugate z^*, so that if $\mathbf{A_1}(m_i, m_{i+1}) = z$, then $\mathbf{A_1}(m_{i+1}, m_i) = z^*$. For the first sample, we impose space-domain relationship with the second and last sensors by means of the complex exponential $e^{j\omega_0\tau}$ and $e^{j(M-1)\omega_0\tau}$. Finally, for the last sample, we use $e^{-j(M-1)\omega_0\tau}$ and $e^{-j\omega_0\tau}$. The space-domain adjacency matrix is given as

$$\mathbf{A_1} = \frac{1}{2}\begin{bmatrix} 0 & e^{j\omega_0\tau} & 0 & \cdots & e^{j(M-1)\omega_0\tau} \\ e^{-j\omega_0\tau} & 0 & e^{j\omega_0\tau} & \ddots & 0 \\ 0 & e^{-j\omega_0\tau} & \ddots & \ddots & \vdots \\ \vdots & \ddots & \ddots & 0 & e^{j\omega_0\tau} \\ e^{-j(M-1)\omega_0\tau} & 0 & \cdots & e^{-j\omega_0\tau} & 0 \end{bmatrix}.$$

The resulting graph is shown on Fig. 2a.

In order to motivate the choice of the adjacency matrix and the division by 2 in the previous equation, we define the snapshot at instant k (see Fig. 1) as vector $\mathbf{x}(k) = [x_1(k) \cdots x_M(k)]^{\mathrm{T}}$, such that, assuming the input signal is a single tone, we can write $\mathbf{x}(k) = \mathbf{A_1}\mathbf{x}(k)$.

B. Time-domain Adjacency Matrix

The set of N samples of the signal captured by the m-th microphone is a time series which can also be interpreted as a directed graph. The idea is similar to that developed for the space-domain graph. We build an $N \times N$ state-transition matrix. In this equation, similarly as in the $\mathbf{A_1}$ adjacency matrix, there are only two nonzero elements per row. Matrix $\mathbf{A_2}$ can be interpreted as the adjacency matrix that contains information about the graph model for each time series. This sparse adjacency matrix holds the neighborhood information between adjacent samples of the signal $x_m(k)$, $x_m(k-1)$ and $x_m(k+1)$, also in function of a complex exponential, $z = e^{-j\omega_0}$. Thus, if $\mathbf{A_2}(n_i, n_j) = z$, then $\mathbf{A_2}(n_j, n_i) = z^*$. For the first sample, we impose their time-domain relationship with the second and the last sample by means of the complex exponential $e^{-j\omega_0}$ and $e^{-j(N-1)\omega_0}$. Finally, for the last sample, we use $e^{j(N-1)\omega_0}$ and $e^{j\omega_0}$. The time-domain adjacency matrix is given as

$$\mathbf{A_2} = \frac{1}{2}\begin{bmatrix} 0 & e^{-j\omega_0} & 0 & \dots & e^{-j(N-1)\omega_0} \\ e^{j\omega_0} & 0 & e^{-j\omega_0} & \ddots & 0 \\ 0 & e^{j\omega_0} & 0 & \ddots & \vdots \\ \vdots & \ddots & \ddots & \ddots & e^{-j\omega_0} \\ e^{j(N-1)\omega_0} & 0 & \cdots & e^{j\omega_0} & 0 \end{bmatrix}.$$

If we define a vector from all samples of $x_m(k)$, $0 \le k < N$, $\mathbf{x}_m = [x_m(0) \cdots x_m(N-1)]^{\mathrm{T}}$, the choice of this adjacency matrix, was motivated by the fact that, assuming again that the input signal $x_m(t)$ is a single cosine, $\mathbf{x}_m = \mathbf{A}_2\mathbf{x}_m$. The time-domain graph for the m-th sensor is depicted in Fig. 2c.

C. The Space-time Graph

Graph products can be used for network modeling [14], image processing [15] and biological computation [16]; more recently, they were proposed as tools for parallelization and vectorization techniques [17]. In this work, we apply the Kronecker product to relate adjacency matrices, $\mathbf{A_1}$ and $\mathbf{A_2}$, computing an adjacency matrix $\mathbf{A}$ corresponding to a space-time graph, whose nodes are shown in Fig. 2b. Given the sizes of matrices $\mathbf{A_1}$ and $\mathbf{A_2}$, $M \times M$ and $N \times N$, respectively, the Kronecker product, an $MN \times MN$ matrix, is denoted by $\mathbf{A}_\otimes = \mathbf{A_2} \otimes \mathbf{A_1}$ and is computed according to [18]. Fig. 2b shows nodes and its relations with other nodes in the graph generated by Kronecker product using matrices $\mathbf{A_1}$ and $\mathbf{A_2}$. Note that the actual graph is directed, so each edge in the figure is actually two edges with opposing directions and complex conjugated weights.

If we stack all available samples (N samples from each of the M microphones) as in

$$\mathbf{x} = \left[\mathbf{x}^{\mathrm{T}}(0) \cdots \mathbf{x}^{\mathrm{T}}(N-1)\right]^{\mathrm{T}}, \tag{1}$$

with $\mathbf{x}(k)$ as previously defined, it is possible, assuming the incoming signal a single cosine $x_m(t)$, to prove that $\mathbf{x}$ is an eigenvector of $\mathbf{A}_\otimes = \mathbf{A_2} \otimes \mathbf{A_1}$ with unit eigenvalue [19], that is, $\mathbf{x} = \mathbf{A}_\otimes\mathbf{x}$.

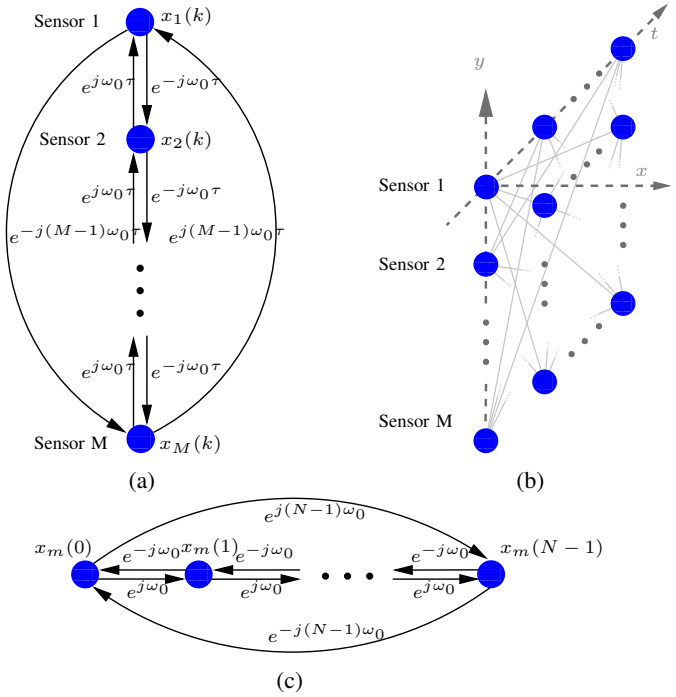

Fig. 2: a) Space-domain graph b) Nodes of the space-time graph. c) Time-domain Graph.

Therefore, $\mathbf{A_2} \otimes \mathbf{A_1}$ is a good candidate for an adjacency matrix of the space-time graph. Conversely, we also claim that $\mathbf{A_1} \otimes \mathbf{A_2}$ would be a possible adjacency matrix in case we form the extended input signal vector as in $\left[\mathbf{x}_1^{\mathrm{T}} \cdots \mathbf{x}_M^{\mathrm{T}}\right]^{\mathrm{T}}$, $\mathbf{x}_m$ as previously defined. Other graph products commonly used in the literature [17] are the Cartesian product $\mathbf{A}_\times$ and the strong product $\mathbf{A}_\boxtimes$ defined, respectively, as $\mathbf{A}_\times = \mathbf{A}_2 \times \mathbf{A}_1 = \mathbf{A}_2 \otimes \mathbf{I}_M + \mathbf{I}_N \otimes \mathbf{A}_1$, and $\mathbf{A}_\boxtimes = \mathbf{A}_2 \boxtimes \mathbf{A}_1 = \mathbf{A}_\otimes + \mathbf{A}_\times$.

The three products have closely related eigendecompositions. Assuming that vector $\mathbf{x}$ is formed from single-tone complex exponentials and defined as in Eq. (1), it is an eigenvector associated with eigenvalue $\lambda = 1$ of both matrices $\mathbf{A_2} \otimes \mathbf{I}_M$ and $\mathbf{I}_N \otimes \mathbf{A_1}$. Therefore the GFT has the same frequency components, regardless the graph product. In this work, We only consider the Kronecker product $\mathbf{A} = \mathbf{A}_\otimes = \mathbf{A_2} \otimes \mathbf{A_1}$ for constructing the space-time adjacency matrix. In this case, matrix $\mathbf{A}$ is not circulant and the space-time graph is not a cyclic graph [20].

IV. GFT applied to DoA estimation

As previously noted, for a single tone incoming signal, vector $\mathbf{x}$ is an eigenvector (with unit eigenvalue) of the space-time adjacency matrix $\mathbf{A}$. Therefore, the spectral decomposition $\mathbf{A} = \mathbf{V}\mathbf{\Lambda}\mathbf{V}^{\mathrm{H}}$ leads to a GFT $\hat{\mathbf{x}} = \mathbf{V}^{\mathrm{H}}\mathbf{x}$ being nonzero only for the position of the unit eigenvalue corresponding to the eigenvector $\mathbf{x}$. This is true provided that matrix $\mathbf{A}$, which is a function of ω_0 and τ, corresponds to the correct frequency and the correct angle of arrival; otherwise, one may not expect that $\mathbf{x}$ is an eigenvector of $\mathbf{A}$. The frequency is assumed correct once the signal is processed through a narrow

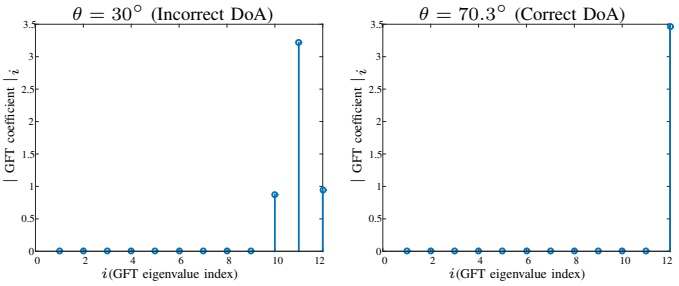

(a) (b)

Fig. 3: GFT representation of an extended signal vector obtained from a 1kH tone impinging on 3×4 standard ULA at 70.3°: (a) multiple peaks when GFT comes from an incorrect DoA, and (b) a single peak when the GFT corresponds to the correct DoA.

bandpass filter, see Fig. 1. The effect of using the correct angle of arrival can be observed in Fig. 3a, where matrix $\mathbf{A}$ was calculated for $\theta = 30°$, whereas the wavefront hits the array at $\theta = 70.3°$. Conversely, for the correct DoA, the energy of $\hat{\mathbf{x}}$ (its norm) is concentrated in one GFT coefficient, as seen in Fig. 3b. This fact motivated us to use an objective function over variable θ, hereinafter referred to as *piquancy function*, defined as $\xi(\theta) = 1/\|\hat{\mathbf{x}}_{-}\|$, where θ varies from $0°$ to $180°$, $\|\hat{\mathbf{x}}_{-}\| = \sqrt{\sum_{i,i\neq i_{\text{eig}}} |\hat{x}_i|^2}$ and i_{eig} is the index of the eigenvector (column of $\mathbf{V}$) associated with the unitary eigenvalue; also the absolute value of $\hat{x}_i$, the ith element of $\hat{\mathbf{x}} = \mathbf{V}^{\text{H}}(\theta)\mathbf{x}$, was normalized such that $|\hat{x}_{i_{\text{eig}}}| = 1$.

We can apply properties of the Kronecker product to simplify the way we obtain the eigenvector matrix $\mathbf{V}$. Letting $\mathbf{A}_1 = \mathbf{V}_1\mathbf{\Lambda}_1\mathbf{V}_1^{\text{H}}$ and $\mathbf{A}_2 = \mathbf{V}_2\mathbf{\Lambda}_2\mathbf{V}_2^{\text{H}}$, if we compute $\mathbf{V}_{\mathbb{K}} = \mathbf{V_2} \otimes \mathbf{V_1}$ and $\mathbf{\Lambda}_{\mathbb{K}} = \mathbf{\Lambda_2} \otimes \mathbf{\Lambda_1}$, the space-time adjacency matrix can be written in a less complex way as $\mathbf{A} = \mathbf{V}_{\mathbb{K}}\mathbf{\Lambda}_{\mathbb{K}}\mathbf{V}_{\mathbb{K}}^{\text{H}}$ [19], [21]. As $\mathbf{V}_2$ is independent of both θ and incoming signal, it can be stored. $\mathbf{V}_1$ is a function of θ but does not depend on the input signal and, therefore, we can store in advance all possible $\mathbf{V}_1(\theta)$. This way the grid search has complexity equivalent to computing the Kronecker product ($\mathbf{V}_{\mathbb{K}} = \mathbf{V_2} \otimes \mathbf{V_1}$) followed by matrix-vector multiplication $\mathbf{V}^{\text{H}}(\theta)\mathbf{x}$ for each value of θ. More efficient methods than grid search could be employed to further decrease computational complexity.

V. Experimental Results

In this section, we consider three scenarios, in all of them we considered a standard ULA with $M = 5$ microphones, $N = 41$ time samples per microphone and $f_s = 8kHz$. In the first scenario we used a sine wave with frequency f_o=2kHz impinging the array from $\theta = 70.3°$. In the second scenario, was used a modulated signal using AM-DSB modulation with the information represented as a 30 Hz sine wave. The last scenario used the same modulated signal as before, but considered 3 multipath signals (same frequency of the interest signal but with -6dB, -8dB and -9dB impinging from $\theta = 20.2°$, $100.7°$ and $60.1°$, respectively) and an interfering signal, with

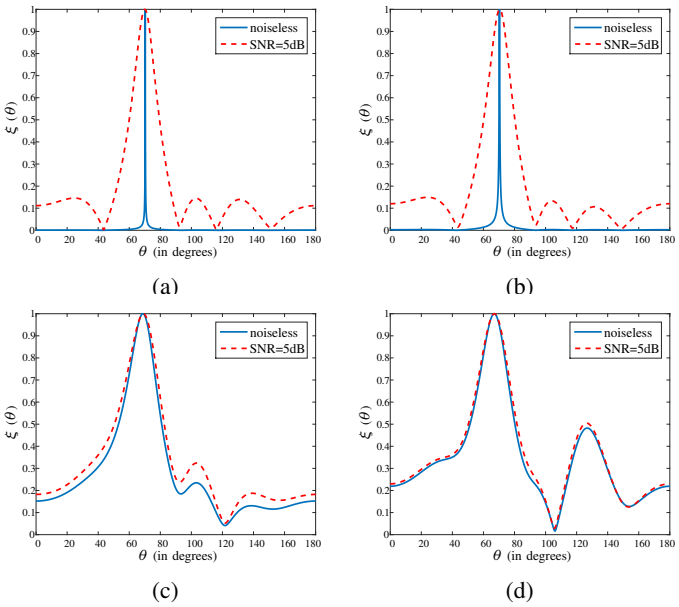

(a) (b) (c) (d)

Fig. 4: Piquancy function (normalized) of a signal with DoA ($\theta = 70.3^o$) noiseless and SNR=5dB: (a) single tone (b) modulated signal (c) modulated signal with multipath (d) similar to the previous one, but including interfering signal.

a frequency different from that of the signal of interest, but inside the range of the bandpass filter, see Fig. 1, with half the power of the signal of interest arriving at $\theta = 120°$.

The graph matching the Kronecker product has $MN = 205$ nodes. For a noiseless signal, it is possible to verify that the method described in Section IV estimates the correct DoA as suggested in Fig. 4a, where the eigenvalue unitary was the last entry in the diagonal matrix $\mathbf{\Lambda}$. Also, in the same figure, we present the piquancy function for a noisy (5dB) signal. In Fig. 4b we show the effect of using a modulated signal instead of a pure tone. Fig. 4c displays the effect of multipath signals, and Fig. 4d exposes the behaviour of piquancy function to the third scenario, in this scenario we can see that GSP method can indicates the existence of a second source (interfering signal) by the presence of another peak in the piquancy function.

By adding normal random noise (AWGN) to the input signal of interest, the performance of the proposed method is comparable to results obtained by classical methods. Fig. 5a shows the root-mean-square error (RMSE) obtained as an average of 1000 independent runs with signal-to-noise ratio (SNR, in dB) equal to 20, 5 and 2. The RMSE was calculated, for each method, computing the difference between each output θ that maximizes the function $\xi(\theta)$ and the reference value ($\theta = 70.3^o$). DoA estimation methods Delay-and-sum (DS), MUSIC, ESPRIT and the proposed GSP-based were evaluated.

As can be seen in Fig. 5a and Fig. 5b the performance using modulated signal is very similar to the pure sine. So, although the theory was developed considering a pure sine as incoming signal it also works for narrowband signals. Furthermore, it

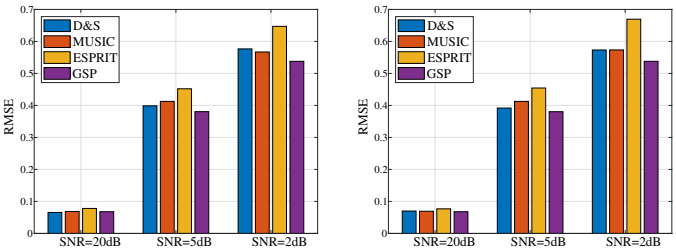

(a) (b)

Fig. 5: RMSE after 1000 independent runs. a) first scenario, single tone b) second scenario, modulated signal.

TABLE I: Performance comparison in third scenario, using a modulated signal, multipaths and interfering signal: RMSE and error variance calculated after 1000 independent runs.

	SNR = 2dB		SNR = 5dB		SNR = 20dB	
	RMSE	Error Variance	RMSE	Error Variance	RMSE	Error Variance
D&S	**3.392**	0.4200	**3.383**	0.211	3.363	0.0063
MUSIC	3.459	0.4493	3.401	**0.1901**	3.383	0.0067
ESPRIT	6.548	2.1926	6.373	0.9716	6.282	0.0275
GSP	3.408	**0.3970**	3.385	0.1996	**0.334**	**0.0060**

is clear that, depending on the SNR, the GSP method may achieve better results than the classical methods tested herein.

The simulation results from the third scenario are depicted in Table I, where we see that, for the application at hand and the objective measures chosen therein, the performance of the proposed algorithm is among the best results compared to classical algorithms in a more harsh scenario including multipath and interference. Another interesting fact is that multipath and interfering signals have larger impact in the RMSE, while noise has larger influence in the error variance.

VI. Conclusion

This paper introduces a new DoA estimation method based on Graph Signal Processing. We propose a graph representation of the spatial shift of the set of sensors such that, for a single sinusoidal input signal, the signal vector corresponds to an eigenvector of the adjacency matrix. The graph representation of the time shift among neighboring samples is such that there is no need for arranging the data in a cyclic buffer where the rightmost sample corresponds to the one to the left of the first sample. We employ the concept of graph product to relate the ULA snapshot and the time series representing the signal received by each sensor. Due to the structure of the proposed space-time graph, the Graph Fourier Transform is used to devise an objective function to be optimized by a line search in order to estimate the DoA. This method favors parallel implementations, more suitable for processing of huge amount of data, but eigenvectors of the adjacency matrix for each DoA can be calculated offline, thereby reducing computational complexity significantly in a non parallel implementation. Simulation results show that the proposed method works well for modulated signals and is suitable for harsh environments, particularly under the presence of multipath and interfering signals.

References

[1] A. Ortega, P. Frossard, J. Kovaevi, J. M. F. Moura, and P. Vandergheynst, "Graph signal processing: Overview, challenges, and applications," *Proceedings of the IEEE*, vol. 106, no. 5, pp. 808–828, May 2018.

[2] Fan Chung, *Spectral Graph Theory*, American Mathematical Society, 1997.

[3] David I. Shuman, Sunil K. Narang, Pascal Frossard, Antonio Ortega, and Pierre Vandergheynst, "The emerging field of signal processing on graphs: Extending high-dimensional data analysis to networks and other irregular domains," *IEEE Signal Processing Magazine*, vol. 30, no. 3, pp. 83–98, May 2013.

[4] A. Sandryhaila and J. M. F. Moura, "Discrete signal processing on graphs," *IEEE Transactions on Signal Processing*, vol. 61, no. 7, pp. 1644–1656, April 2013.

[5] X. Zhu and M. Rabbat, "Graph spectral compressed sensing for sensor networks," in *2012 IEEE International Conference on Acoustics, Speech and Signal Processing (ICASSP)*, March 2012, pp. 2865–2868.

[6] S. Lafon and A. B. Lee, "Diffusion maps and coarse-graining: a unified framework for dimensionality reduction, graph partitioning, and data set parameterization," *IEEE Transactions on Pattern Analysis and Machine Intelligence*, vol. 28, no. 9, pp. 1393–1403, Sept 2006.

[7] Ronald R. Coifman and Stéphane Lafon, "Diffusion maps," *Applied and Computational Harmonic Analysis*, vol. 21, no. 1, pp. 5–30, 2006, Special Issue: Diffusion Maps and Wavelets.

[8] R. Talmon, I. Cohen, and S. Gannot, "Supervised source localization using diffusion kernels," in *2011 IEEE Workshop on Applications of Signal Processing to Audio and Acoustics (WASPAA)*, Oct 2011, pp. 245–248.

[9] Ralph Otto Schmidt, *A Signal Subspace Approach to Multiple Emitter Location and Spectral Estimation*, Ph.D. thesis, Stanford University (Department of Electrical Engineering), 1981.

[10] R. Roy and T. Kailath, "Esprit-estimation of signal parameters via rotational invariance techniques," *IEEE Transactions on Acoustics, Speech, and Signal Processing*, vol. 37, no. 7, pp. 984–995, Jul 1989.

[11] A. Sandryhaila and J. M. F. Moura, "Discrete signal processing on graphs: Frequency analysis," *IEEE Transactions on Signal Processing*, vol. 62, no. 12, pp. 3042–3054, June 2014.

[12] Lloyd N. Trefethen and David Bau, III, *Numerical Linear Algebra*, SIAM, 1997.

[13] H.L. Van Trees, *Optimum Array Processing: Part IV of Detection, Estimation, and Modulation Theory*, Detection, Estimation, and Modulation Theory. Wiley, 2004.

[14] Jure Leskovec, Deepayan Chakrabarti, Jon Kleinberg, Christos Faloutsos, and Zoubin Ghahramani, "Kronecker graphs: An approach to modeling networks," *J. Mach. Learn. Res.*, vol. 11, pp. 985–1042, Mar. 2010.

[15] D. E. Dudgeon and R. M. Mersereau, *Discrete-Time Signal Processing*, Prentice Hall, 1983.

[16] M. Hellmuth, D. Merkle, and M. Middendorf, "Extended shapes for the combinatorial design of rna sequences," *Int. J. of Computational Biology and Drug Design*, vol. 2, no. 4, pp. 371–384, 2009.

[17] A. Sandryhaila and J. M. F. Moura, "Big data analysis with signal processing on graphs: Representation and processing of massive data sets with irregular structure," *IEEE Signal Processing Magazine*, vol. 31, no. 5, pp. 80–90, Sept 2014.

[18] R. Hammack, W. Imrich, and S. Klavzar, *Handbook of Product Graphs*, CRC Press, 2 edition, 2011.

[19] R. A. Horn and C. R. Johnson, *Topics in Matrix Analysis*, Cambridge University Press, 1991.

[20] R. Balakrishnan, G. Sethuraman, and R.J. Wilson, *Graph Theory and Its Applications*, Narosa Publishing House, 2004.

[21] Kathrin Schcke, "On the kronecker product," https://www.math.uwaterloo.ca/~hwolkowi/henry/reports/kronthesisschaecke04.pdf, 2004.